

Thermodynamic stability of alkali metal/zinc double-cation borohydrides at low temperatures

Tran Doan Huan,¹ Maximilian Amsler,¹ Riccardo Sabatini,² Vu Ngoc Tuoc,³ Nam Ba Le,^{3,4} Lilia M. Woods,⁴ Nicola Marzari,² and Stefan Goedecker^{1,*}

¹*Department of Physics, Universität Basel, Klingelbergstrasse 82, 4056 Basel, Switzerland*

²*Theory and Simulation of Materials, École Polytechnique Fédérale de Lausanne, Station 12, 1015 Lausanne, Switzerland*

³*Institute of Engineering Physics, Hanoi University of Science and Technology, 1 Dai Co Viet Road, Hanoi, Vietnam*

⁴*Department of Physics, University of South Florida, 4202 E. Fowler Ave., Tampa, FL 33620, USA*

(Dated: April 16, 2013)

We study the thermodynamic stability at low temperatures of a series of alkali metal/zinc double-cation borohydrides, including $\text{LiZn}(\text{BH}_4)_3$, $\text{LiZn}_2(\text{BH}_4)_5$, $\text{NaZn}(\text{BH}_4)_3$, $\text{NaZn}_2(\text{BH}_4)_5$, $\text{KZn}(\text{BH}_4)_3$, and $\text{KZn}_2(\text{BH}_4)_5$. While $\text{LiZn}_2(\text{BH}_4)_5$, $\text{NaZn}(\text{BH}_4)_3$, $\text{NaZn}_2(\text{BH}_4)_5$ and $\text{KZn}(\text{BH}_4)_3$ were recently synthesized, $\text{LiZn}(\text{BH}_4)_3$ and $\text{KZn}_2(\text{BH}_4)_5$ are hypothetical compounds. Using the minima-hopping method, we discover two new lowest-energy structures for $\text{NaZn}(\text{BH}_4)_3$ and $\text{KZn}_2(\text{BH}_4)_5$ which belong to the $C2/c$ and $P2$ space groups, respectively. These structures are predicted to be both thermodynamically stable and dynamically stable, implying that their existence may be possible. On the other hand, the lowest-energy $P1$ structure of $\text{LiZn}(\text{BH}_4)_3$ is predicted to be unstable, suggesting a possible reason elucidating why this compound has not been experimentally identified. In exploring the low-energy structures of these compounds, we find that their energetic ordering is sensitive to the inclusion of the van der Waals interactions. We also find that a proper treatment of these interactions, e.g., as given by a non-local density functional such as vdw-DF2, is necessary to address the stability of the low-energy structures of these compounds.

PACS numbers: 61.66.-f, 63.20.dk, 61.05.cp

I. INTRODUCTION

Hydrogen is a promising alternative to fossil fuels as it can provide a high density of clean energy. To use hydrogen as a fuel, a safe and efficient storage method is crucial, especially for mobile applications.^{1–4} Many solid state materials, including complex borohydrides $M(\text{BH}_4)_m$, have been studied for hydrogen-storage purposes (here M is a metal of valence m). However, none of these compounds currently meets all the requirements for a hydrogen storage medium. For examples, the dehydrogenation of alkaline-earth metal borohydrides $M(\text{BH}_4)_2$ is generally too slow, while alkali metal borohydrides $MB\text{H}_4$ are thermodynamically too stable. Attempts to improve their performance, e.g., by using additives, by partial substitutions, or by subjecting them to confinement at the nanoscale, have been met by limited success.⁵

A large number of double-cation borohydrides $M_iN_j(\text{BH}_4)_{mi+nj}$ were recently synthesized and proposed as candidates of hydrogen-storage materials (N is also a metal of valence n). Several examples of such compounds include Li/K borohydrides,⁶ Li/Ca borohydrides,⁷ Li/Sc borohydrides,⁸ Na/Sc borohydrides,⁹ K/Sc borohydrides,¹⁰ Na/Al borohydrides,¹¹ K/Mn and K/Mg borohydrides,¹² K/Y borohydrides,¹³ Li/Zn and Na/Zn borohydrides,^{14–16} K/Zn borohydrides.¹⁷ These compounds, whose hydrogen storage capacity is relatively high, were suggested to have decomposition temperatures lying somewhere between those of the corresponding single-cation borohydrides.^{4,6,9,12,14,16,17} Such compelling feature would allow for the adjustment of the decomposition

temperature by selecting an appropriate cation combination. Theoretical studies on these newly developed materials were subsequently carried out.^{12,18–22}

In this work, we consider a series of compounds of Li/Zn, Na/Zn, and K/Zn double-cation borohydrides of which $\text{LiZn}_2(\text{BH}_4)_5$, $\text{NaZn}(\text{BH}_4)_3$, $\text{NaZn}_2(\text{BH}_4)_5$ and $\text{KZn}(\text{BH}_4)_3$ were experimentally synthesized.^{14–17} At ambient conditions, $\text{LiZn}_2(\text{BH}_4)_5$ crystallizes in an orthorhombic $Cmca$ (no. 64) phase as first determined by powder x-ray diffraction (XRD) analysis¹⁴ and then refined by powder neutron diffraction, Raman and NMR spectroscopy.^{15,16} Next, $\text{NaZn}(\text{BH}_4)_3$ and $\text{NaZn}_2(\text{BH}_4)_5$ were found to be in two phases which both belong to the monoclinic $P2_1/c$ space group (no. 14).^{14,15} At 100K, $\text{KZn}(\text{BH}_4)_3$ was determined to crystallize in a rhombohedral $R\bar{3}$ phase (no. 146).¹⁷ Two related hypothetical compounds that are also considered in this work are $\text{LiZn}(\text{BH}_4)_3$ and $\text{KZn}_2(\text{BH}_4)_5$. While both of them have not experimentally been observed yet, a $P2_1/c$ phase (no. 14) and a $P1$ (no. 1) phase of $\text{LiZn}(\text{BH}_4)_3$ were theoretically proposed in Refs. 15 and 18, respectively. No information on $\text{KZn}_2(\text{BH}_4)_5$ is available in the literature.

Some of the structural phases experimentally proposed for these compounds were recently suggested to be thermodynamically unstable at 0K by a theoretical study based on *ab initio* calculations.¹⁸ In particular, the unrefined $Cmca$ phase of $\text{LiZn}_2(\text{BH}_4)_5$ proposed by Ref. 14 was suggested to be slightly unstable with respect to the decomposition into $\text{Zn}(\text{BH}_4)_2$ and the $P1$ phase of $\text{LiZn}(\text{BH}_4)_3$. Furthermore, the $P2_1/c$ phase of $\text{NaZn}(\text{BH}_4)_3$ was found¹⁸ to be unstable with respect to the decomposition into $\text{NaBH}_4 + \text{Zn}(\text{BH}_4)_2$. However,

it turns out that the correct stability of $\text{LiZn}_2(\text{BH}_4)_5$ has to be examined by using the $Cmca$ phase which was refined by Refs. 15,16. Also, because the refined $Cmca$ phase of $\text{LiZn}_2(\text{BH}_4)_5$ was noted¹⁸ to be lower in energy than the unrefined $Cmca$ phase, the conclusion of Ref. 18 that the $P1$ structure of $\text{LiZn}(\text{BH}_4)_3$ is stable has to be re-examined. In addition, the recent proposal of the $P1$ phase of $\text{NaZn}(\text{BH}_4)_3$,¹⁸ which is more stable than the experimentally synthesized $P2_1/c$ phase,¹⁴ suggests that unexplored low-energy structures of the Li/Zn and Na/Zn borohydrides may exist. Finally, as $\text{KZn}(\text{BH}_4)_3$ was synthesized very recently,¹⁷ it is worth to explore the (additional) possible low-energy structures of $\text{KZn}(\text{BH}_4)_3$ and its related compounds, e.g., $\text{KZn}_2(\text{BH}_4)_5$.

These above open issues on the thermodynamic stability of the Li/Zn, Na/Zn, and K/Zn borohydrides are examined in this work. In order to discuss the stability of these compounds, we search and discover a large number of low-energy structures using the minimahopping method.^{23,24} Van der Waals (vdW) interactions, which were recently shown²⁵ to be important in describing the stabilization of the low-energy structures of $\text{Mg}(\text{BH}_4)_2$, is properly considered using vdW density-functional theory.^{26–29} Finally, we study the thermodynamical stability of these compounds at finite temperatures by determining the vibrational free energy from the phonon frequency spectra of the examined low-energy structures within the harmonic approximation.

II. METHODS

First-principles calculations reported in this work were performed at the level of the density functional theory (DFT)^{30,31} within the Perdew-Burke-Ernzerhof (PBE) generalized gradient approximation.³² The projected augmented wave formalism³³ as implemented in *Vienna Ab Initio Simulation Package* (VASP)^{34–36} was employed. The valence electron configurations of Zn, B, Li, Na, and K used for calculations are $3d^{10}4s^2$, $2s^22p^1$, $1s^22s^1$, $2s^22p^63s^1$ and $3s^23p^64s^1$, respectively. The convergence of the DFT energy $E_{\text{DFT}}^{\text{PBE}}$ was ensured by a Monkhorst-Pack \mathbf{k} -point mesh³⁷ from $5 \times 5 \times 5$ to $9 \times 9 \times 9$, depending on the simulation cell sizes, for sampling the Brillouin zone and a kinetic energy plane wave cutoff of 900 eV. Atomic and cell variables were simultaneously relaxed until the residual forces were smaller than 0.01 eV/Å. The effect of vdW interactions of all the examined structures was explored in separate calculations using the modified Langreth-Lundqvist non-local density functional (vdW-DF2)^{26–29} as implemented in the PWSCF code of the QUANTUM ESPRESSO distribution.³⁸ The rPW86 pseudopotentials^{39,40} of the PsLibrary at an energy cutoff of 80 Ry were used in the calculations for the DFT energy $E_{\text{DFT}}^{\text{vdW}}$, taking into account the vdW interactions. The space groups of the examined structures were determined by FINDSYM⁴¹ while some figures were

prepared by VESTA.⁴²

We tested our computational scheme by optimizing the experimentally reported structures of $\text{LiZn}_2(\text{BH}_4)_5$,^{14–16} $\text{NaZn}(\text{BH}_4)_3$,^{14,15} $\text{NaZn}_2(\text{BH}_4)_5$,^{14,15} $\text{KZn}(\text{BH}_4)_3$,¹⁷ LiBH_4 ,⁴³ NaBH_4 ,⁴⁴ and KBH_4 .^{45,46} The optimized structures are summarized in Table I, showing that the $Cmca$ structure of $\text{LiZn}_2(\text{BH}_4)_5$ obtained from the PBE optimization agrees very well with experimental data.¹⁶ Moreover, our results for the $P2_1/c$ phases of $\text{NaZn}(\text{BH}_4)_3$ and $\text{NaZn}_2(\text{BH}_4)_5$ are consistent with those reported in Ref. 18, which are generally in good agreement with the experimental values,¹⁴ except for some discrepancies on b of $\text{NaZn}(\text{BH}_4)_3$, and on a of $\text{NaZn}_2(\text{BH}_4)_5$. While the origin of these discrepancies is still unclear,⁴⁷ we note that a similar discrepancy on b of the $P2_1/c$ phase of $\text{NaZn}(\text{BH}_4)_3$ was already reported in Ref. 18. In addition, c calculated for the $R3$ phase of $\text{KZn}(\text{BH}_4)_3$ is about 10% larger than the experimental value.¹⁷ Presumably, this deviation may come from the finite temperature (100K) at which the $\text{KZn}(\text{BH}_4)_3$ samples were analyzed and/or the fact that a , b , and c were all fixed in the DFT calculations subsequently performed to confirm the space group $R3$ determined experimentally.^{17,48} For LiBH_4 , NaBH_4 , and KBH_4 , the calculated results agree very well with the experimentally measured values. With vdW-DF2, as also shown by Table I, the agreement between the calculated results and the experimental data is improved. Similar to the PBE results, the lattice parameters of $\text{LiZn}_2(\text{BH}_4)_5$, LiBH_4 , NaBH_4 , and KBH_4 optimized with vdW-DF2 agree well with the experimental values. Furthermore, the discrepancies previously observed for $\text{NaZn}(\text{BH}_4)_3$, $\text{NaZn}_2(\text{BH}_4)_5$, and $\text{KZn}(\text{BH}_4)_3$ with the PBE optimization are strongly diminished. These observations clearly show that the long-ranged vdW interactions in the examined structures can be well captured by the non-local vdW-DF2 functional used in this work.

Unconstrained searches for low-energy structures of the examined compounds were performed by the minimahopping method (MHM).^{23,24} In this method, the PBE energy landscapes are explored by consecutive short molecular dynamics steps followed by local geometry relaxations. The initial velocities for the molecular dynamics runs are chosen approximately along soft mode directions, allowing efficient escapes from local minima, and aiming towards the global minimum. This method was successfully applied in a wide range of material structure predictions.^{49–58} Some of the theoretical predictions by MHM on neutral Si clusters and four-fold defects in silicon were recently confirmed by experiments.^{59,60}

Phonon frequency spectra of the examined structures were calculated with the PBE functional using the PHONOPY package.^{61,62} Given a sufficiently large relaxed super cell, finite atomic displacements with an amplitude of 0.01 Å were introduced. The atomic forces within the super cells were calculated with VASP and the phonon frequencies were then calculated from the dynamical matrix, given in terms of the force constants.⁶² The longi-

TABLE I: Geometrical parameters (lattice parameters a , b , and c in Angstrom, angle β in degree, and volume difference ΔV in percent) obtained by computationally optimizing the experimentally-reported low-energy structures of the examined compounds and several related compounds. References are given for the experimental data, which are presented for the comparison purpose.

Compound	Space group	Calculations with PBE					Calculations with vdW-DF2					Experiments				
		$a(\text{\AA})$	$b(\text{\AA})$	$c(\text{\AA})$	$\beta(^{\circ})$	$\Delta V(\%)$	$a(\text{\AA})$	$b(\text{\AA})$	$c(\text{\AA})$	$\beta(^{\circ})$	$\Delta V(\%)$	$a(\text{\AA})$	$b(\text{\AA})$	$c(\text{\AA})$	$\beta(^{\circ})$	Ref.
$\text{LiZn}_2(\text{BH}_4)_5$	$Cmca$	8.63	18.03	15.43	90	0.9	8.76	17.62	15.78	90	2.4	8.62	17.90	15.41	90	[16]
$\text{NaZn}(\text{BH}_4)_3$	$P2_1/c$	8.02	5.38	18.57	101.5	14.3	8.84	4.65	17.14	100.0	1.1	8.27	4.52	18.76	101.7	[14]
$\text{NaZn}_2(\text{BH}_4)_5$	$P2_1/c$	10.45	16.19	9.06	112.4	6.4	9.07	17.05	9.36	112.2	1.7	9.40	16.64	9.14	112.7	[14]
$\text{KZn}(\text{BH}_4)_3$	$R3$	7.80	7.80	12.24	90	16.5	7.78	7.78	11.88	90	12.6	7.63	7.63	10.98	90	[17]
LiBH_4	$Pnma$	7.30	4.39	6.60	90	-2.4	6.96	4.54	6.72	90	-2.1	7.18	4.44	6.80	90	[43]
NaBH_4	$P4_2/nmc$	4.34	4.34	5.88	90	0.6	4.36	4.36	5.86	90	1.2	4.33	4.33	5.87	90	[44]
KBH_4	$P4_2/nmc$	4.76	4.76	6.68	90	0.6	4.72	4.72	6.60	90	-3.4	4.77	4.77	6.69	90	[45]

tudinal optical/transverse optical splitting was not considered because its effects were reported to be negligible for a wide variety of hydrides.^{63,64}

For a double-cation borohydride, we computed the formation energy to examine if it is stable with respect to the decomposition into the corresponding single-cation borohydrides and related compounds. As an example, the formation energy of $\text{LiZn}_2(\text{BH}_4)_5$ was determined by

$$\Delta F = F[\text{LiZn}_2(\text{BH}_4)_5] - \{xF[\text{LiBH}_4] + (1-x)F[\text{Zn}(\text{BH}_4)_2]\} \quad (1)$$

where $x = 2/3$ is the Zn cation composition of $\text{LiZn}_2(\text{BH}_4)_5$. Here, $F[\text{LiZn}_2(\text{BH}_4)_5]$, $F[\text{LiBH}_4]$, and $F[\text{Zn}(\text{BH}_4)_2]$ are the free energies of one formula unit of $\text{LiZn}_2(\text{BH}_4)_5$, LiBH_4 , and $\text{Zn}(\text{BH}_4)_2$, respectively. The examined structure of $\text{LiZn}_2(\text{BH}_4)_5$ is stable if ΔF is negative; otherwise, it would decompose into LiBH_4 and $\text{Zn}(\text{BH}_4)_2$. At finite temperature T , the vibrational free energies were determined within the harmonic approximation from the phonon frequency spectra of the examined structures. The formation energy was also calculated from $E_{\text{DFT}}^{\text{vdW}}$, i.e., the DFT energies of the structures, taken into account the vdW interactions. To determine the formation energies ΔF according to Eq. 1, we used the $I4_122$ phase (no. 98) of $\text{Zn}(\text{BH}_4)_2$,^{18,57,65,66} the $Pnma$ phase (no. 62) of LiBH_4 ,⁴³ and the $P4_2/nmc$ phase (no. 137) of both NaBH_4 and KBH_4 .^{44,46,67}

III. LOW-TEMPERATURE STRUCTURES OF ALKALI METAL/ZINC DOUBLE-CATION BOROHYDRIDES

We searched for low-energy structures of $\text{LiZn}(\text{BH}_4)_3$, $\text{NaZn}(\text{BH}_4)_3$, $\text{KZn}(\text{BH}_4)_3$, $\text{LiZn}_2(\text{BH}_4)_5$, $\text{NaZn}_2(\text{BH}_4)_5$, and $\text{KZn}_2(\text{BH}_4)_5$ by using the minima-hopping method. For the first three compounds, we performed searches for 1 f.u. (17 atoms) and 2 f.u. (34 atoms) while for the last three compounds, searches were performed with 1 f.u. (28 atoms). Starting from random input structures, we discovered a large number of new low-energy structures for these compounds. Additional searches were

also performed by relaxing several lowest-energy structures discovered for each compound after replacing their cations by the cations of other appropriate species. Our MHM runs were performed with the PBE functional and the structures discovered were then examined using the vdW-DF2 functional.

We show in Table II the densities and the formation energies, determined with PBE and vdW-DF2, of all the structures discovered together with those already reported in the literature. We note that our results for $\Delta F_{\text{DFT}}^{\text{PBE}}$ for the $P1$ phase of $\text{LiZn}(\text{BH}_4)_3$ and the unrefined $Cmca$ phase of $\text{LiZn}_2(\text{BH}_4)_5$ are consistent with those reported by Ref. 18. The crystallographic information of all the structures we discovered can be found in the Supplemental Material.⁶⁸ Simulated XRD patterns performed by FULLPROF⁶⁹ are also shown in the Supplemental Material,⁶⁸ indicating that the low-energy structures reported in this work are different from those already reported in the literature.

A. Lithium/zinc borohydrides

We optimized the refined $Cmca$ structure of $\text{LiZn}_2(\text{BH}_4)_5$ and found that this structure is thermody-

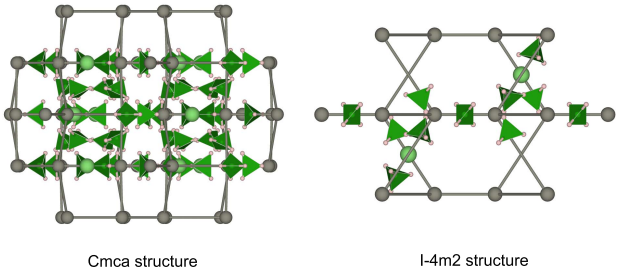


FIG. 1: (Color online) $Cmca$ (left) and $I\bar{4}m2$ (right) phases of $\text{LiZn}_2(\text{BH}_4)_5$. Lithium and zinc atoms are shown by green and gray spheres while $[\text{BH}_4]^-$ complex anions are shown by green tetrahedra. Zn-Zn interlinked “bonds” are used as guides for the eyes.

TABLE II: Summary of the available structures of alkali metal/zinc double cation borohydrides. $\Delta F_{\text{DFT}}^{\text{PBE}}$, $\Delta F_{0\text{K}}^{\text{PBE}}$, $\Delta F_{100\text{K}}^{\text{PBE}}$, and $F_{\text{DFT}}^{\text{vdW}}$, given in kJ/mol cation, are the energies of formation determined from E_{DFT} , $F_{0\text{K}}$, $F_{100\text{K}}$, and $E_{\text{DFT}}^{\text{vdW}}$, respectively. These structures are indicated by their space groups. Densities ρ are given in g/cm³. References are shown for structures not originating from this work.

Compounds	Space group (no.)	ρ (g/cm ³)	$\Delta F_{\text{DFT}}^{\text{PBE}}$	$\Delta F_{0\text{K}}^{\text{PBE}}$	$\Delta F_{100\text{K}}^{\text{PBE}}$	$\Delta F_{\text{DFT}}^{\text{vdW}}$	References
$\text{LiZn}(\text{BH}_4)_3$	$P1$ (1)	0.80	-6.70	-6.89	-7.45	-4.95	[18]
$\text{LiZn}_2(\text{BH}_4)_5$	$Cmca$ (64)	1.18	-10.14	-10.67	-10.61	-19.05	[15,16]
	$I\bar{4}m2$ (119)	0.57	-11.70	-12.96	-13.59	-1.08	
	$P2_1/c$ (14)	1.28	-6.55	-8.43	-8.74	-4.90	[14]
$\text{NaZn}(\text{BH}_4)_3$	$P1$ (1)	0.91	-7.83	-9.25	-9.92	-4.29	[18]
	$C2/c$ (15)	1.00	-10.90	-11.76	-12.05	-9.56	
	$P2_1/c$ (14)	1.15	-12.08	-13.91	-14.58	-11.47	[16]
$\text{NaZn}_2(\text{BH}_4)_5$	$I\bar{4}m2$ (119)	0.54	-11.87	-13.58	-14.87	1.90	
	$R3$ (146)	1.15	-7.31	-9.28	-10.21	-8.86	[17]
	$P6_3/m$ (176)	1.05	-11.08	-12.60	-13.32	-5.10	
$\text{KZn}(\text{BH}_4)_3$	$P2$ (3)	1.09	-8.84	-10.75	-11.39	-10.97	

namically more stable than the unrefined $Cmca$ structure by $\simeq 7.8$ kJ/mol cation. Additionally, from the MHM searches for $\text{LiZn}_2(\text{BH}_4)_5$, we discovered a new tetragonal $I\bar{4}m2$ structure (no. 119), which is more stable than the refined $Cmca$ structure by $\simeq 1.5$ kJ/mol cation. Further calculations with the PBE functional indicated that $I\bar{4}m2$ is the thermodynamically most stable structure of $\text{LiZn}_2(\text{BH}_4)_5$ at temperatures up to 100K (see Table II). While the $Cmca$ structure consists of two identical interpenetrated three-dimensional (3D) frameworks,^{14–16} the $I\bar{4}m2$ structure consists one of these two frameworks with differences in the sequence of Zn atoms and Li atoms. Therefore, it is not surprising that the $I\bar{4}m2$ structures

has a very low density with $\rho = 0.57$ g \times cm⁻³, about one half of the density $\rho = 1.18$ g \times cm⁻³ of the $Cmca$ structure. An illustration for the $Cmca$ and $I\bar{4}m2$ structures is given in Fig. 1, clearly showing the difference in the geometry and density of the $Cmca$ and $I\bar{4}m2$ structures. The density of phonon states of the $I\bar{4}m2$ structure is plotted in Fig. 2(a), indicating that this structure is dynamically stable because no phonon mode with imaginary frequencies was observed in the whole Brillouin zone.

For the hypothetical compound $\text{LiZn}(\text{BH}_4)_3$, we optimized the $P2_1/c$ and $P1$ structures which were theoretically proposed in Refs. 15 and 18, respectively. We found that for the $P1$ structure, $\Delta F_{\text{DFT}}^{\text{PBE}} \simeq -6.7$ kJ/mol cation while for the $P2_1/c$ structure, $\Delta F_{\text{DFT}}^{\text{PBE}} \simeq 19$ kJ/mol cation. The positive formation energy of the $P2_1/c$ structure hints that this structure is unstable and is an incorrect structural model.⁴⁸ On the other hand, $P1$ is the lowest-energy structure of $\text{LiZn}(\text{BH}_4)_3$, as also confirmed by the MHM runs we performed for this hypothetical compound. The $P1$ structure is dynamically stable, as demonstrated by its density of phonon states shown in Fig. 2(b).

We then examined the thermodynamic stability of the $P1$ structure of $\text{LiZn}(\text{BH}_4)_3$ and the $Cmca$ and the $I\bar{4}m2$ structures of $\text{LiZn}_2(\text{BH}_4)_5$ based on the convex hull constructed from the the formation energies of the thermodynamically most stable structures calculated at 0K and 100K with the PBE functional. Fig. 3(a) shows that in agreement with the conclusion of Ref. 18, the unrefined $Cmca$ phase is unstable with respect to the decomposition into $\text{LiZn}(\text{BH}_4)_3$ and $\text{Zn}(\text{BH}_4)_2$. Because the refined $Cmca$ and $I\bar{4}m2$ structures of $\text{LiZn}_2(\text{BH}_4)_5$ are well lower in energy than the unrefined $Cmca$ phase, they remain thermodynamically stable at temperatures up to 100K [see Figs. 3(a)–(c)]. The $P1$ structure of $\text{LiZn}(\text{BH}_4)_3$, on the other hand, is always unstable and would decompose into LiBH_4 and $\text{LiZn}_2(\text{BH}_4)_5$ within this temperature range.

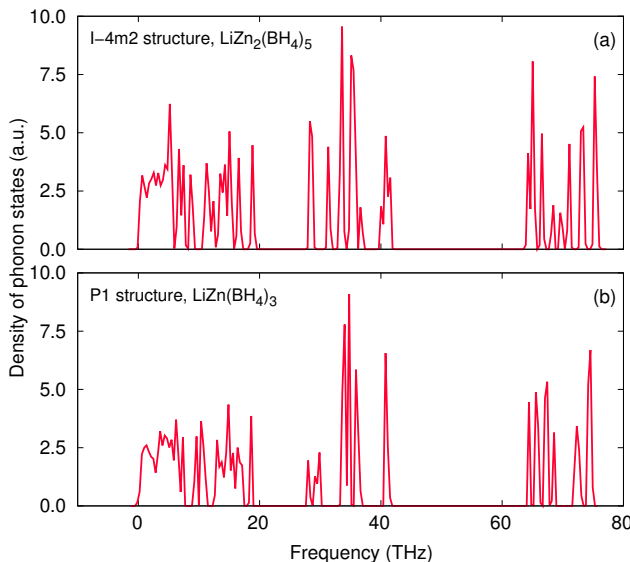


FIG. 2: (Color online) Density of phonon states of (a) the $I\bar{4}m2$ structure of $\text{LiZn}_2(\text{BH}_4)_5$ and (b) the $P1$ structure of $\text{LiZn}(\text{BH}_4)_3$.

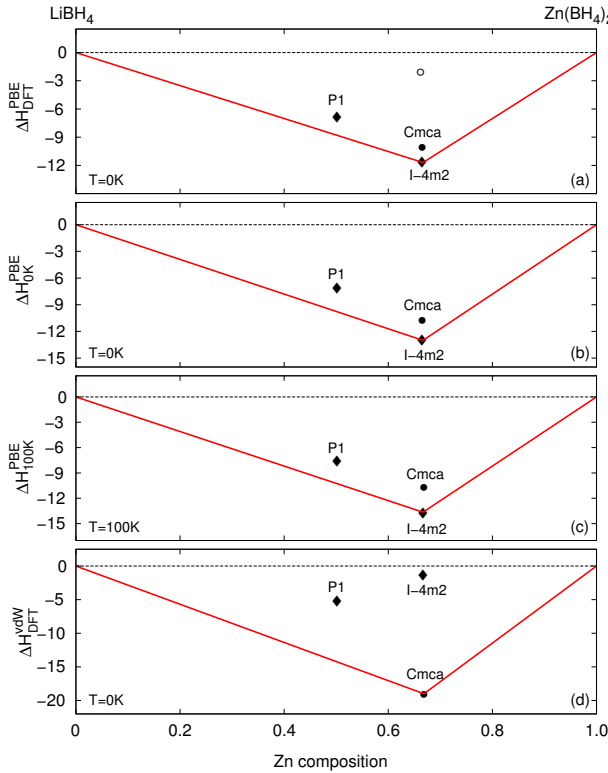


FIG. 3: (Color online) Formation energies $\Delta F_{\text{DFT}}^{\text{PBE}}$, $\Delta F_{0\text{K}}^{\text{PBE}}$, $\Delta F_{100\text{K}}^{\text{PBE}}$, and $\Delta F_{\text{DFT}}^{\text{vdW}}$ (in units of kJ/mol cation) of Li/Zn double-cation borohydrides shown vs. x , the Zn composition of the compounds. For $\text{LiZn}(\text{BH}_4)_3$, $x = 1/2$ while for $\text{LiZn}_2(\text{BH}_4)_5$, $x = 2/3$. The structures studied are indicated by symbols with the space groups nearby. Diamonds/circles are used for theoretically-predicted/experimentally-reported phases. Open circle represents the *unrefined* Cmca structure of $\text{LiZn}_2(\text{BH}_4)_5$. Constructed from the thermodynamically most stable structures, the red-solid lines form a convex hull, above which all structures are unstable.

Figs. 3(a)-(c) demonstrate that at temperatures up to 100K, lattice vibrations have essentially no effect on the energetic ordering. Therefore, it is expected that the formation energy $\Delta F_{\text{DFT}}^{\text{vdW}}$ determined from $E_{\text{DFT}}^{\text{vdW}}$ can be used to establish more accurately the stability of these structures. Fig. 3(d) shows that by considering the vdW interactions, the energetic ordering of the $\bar{I}4m2$ and the Cmca phases of $\text{LiZn}_2(\text{BH}_4)_5$ was reverted. In particular, the Cmca phase is thermodynamically more stable than the $\bar{I}4m2$ phase by $\simeq 18\text{ kJ/mol cation}$ while the $P1$ phase of $\text{LiZn}(\text{BH}_4)_3$ is, again, unstable and would decompose into LiBH_4 and $\text{LiZn}_2(\text{BH}_4)_5$. The instability of the $P1$ phase, as shown in Fig. 3(a)-(d), may be the reason why attempts to experimentally identify $\text{LiZn}(\text{BH}_4)_3$ have failed.^{14,15}

We suggest that the significant role of the vdW interactions in determining the energetic ordering of the Cmca and the $\bar{I}4m2$ structures can be traced back to the difference in the number of 3D frameworks between them.

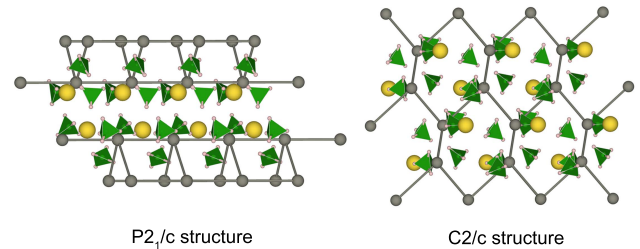


FIG. 4: (Color online) Two low-energy structures of $\text{NaZn}(\text{BH}_4)_3$: $P2_1/c$ (left) and $C2/c$ (right). Sodium and zinc atoms are shown by yellow and gray spheres while $[\text{BH}_4]^-$ complex anions are shown by green tetrahedra.

Because there are no bonds between the two 3D frameworks of the Cmca structure¹⁴⁻¹⁶ while the $\bar{I}4m2$ structure has only one 3D framework, they are almost similar in their energies at the PBE level. However, in the vdW-DF2 calculations, long-ranged interactions between the two frameworks of the Cmca structure can be captured, lowering its energy compared to that of the $\bar{I}4m2$ structure. This behavior is similar to that reported by Ref. 25 where it was argued that the PBE functional artificially stabilizes structures of $\text{Mg}(\text{BH}_4)_2$ with unusually low densities, and a treatment within non-local density functionals such as vdW-DF would be a solution to the problem. In this work, we show that to access the stability of $\text{LiZn}_2(\text{BH}_4)_5$ at low temperatures, it is obviously desirable to properly incorporate the vdW interactions by using a non-local density functional such as vdW-DF2.

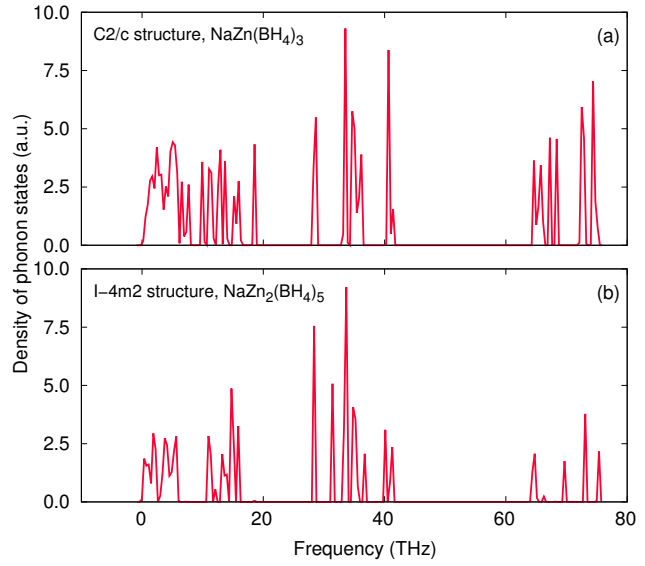


FIG. 5: (Color online) Density of phonon states of (a) the $C2/c$ structure of $\text{NaZn}(\text{BH}_4)_3$ and (b) the $\bar{I}4m2$ structure of $\text{NaZn}_2(\text{BH}_4)_5$.

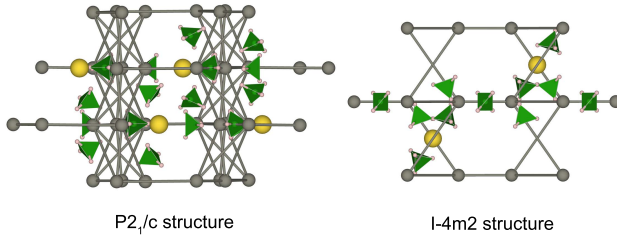


FIG. 6: (Color online) Two low-energy phases of $\text{NaZn}_2(\text{BH}_4)_5$: $P2_1/c$ (left) and $I\bar{4}m2$ (right). Sodium and zinc atoms are shown by yellow and gray spheres while $[\text{BH}_4]^-$ complex anions are shown by green tetrahedra.

B. Sodium/zinc borohydrides

For $\text{NaZn}(\text{BH}_4)_3$, the experimentally observed $P2_1/c$ structure was theoretically predicted¹⁸ to be thermodynamically unstable at 0K. A new $P1$ structure was then proposed¹⁸ to be lower in energy than the $P2_1/c$ structure. Using the MHM, we discovered a new monoclinic $C2/c$ structure (no. 15), which is lower than the $P1$ structure by $\simeq 3\text{kJ/mol}$ cation. Our further results calculated with the PBE functional indicate that $C2/c$ is the thermodynamically most stable structure at temperatures up to 100 K. The $C2/c$ phase, of which the density is $\rho = 1.00 \text{ g} \times \text{cm}^{-3}$, is slightly lighter than the $P2_1/c$ phase with $\rho = 1.28 \text{ g} \times \text{cm}^{-3}$. As an illustration, the geometries of the $P2_1/c$ and $C2/c$ phases are shown in Figure 4. The phonon spectra of these phases were also calculated, indicating that both the proposed ($P1$ and $C2/c$) phases are dynamically stable. For more information, we show in Fig. 5(a) the density of phonon states of the $C2/c$ phase while the density of phonon states of the $P1$ phase can be found in the Supplemental Material.⁶⁸

$\text{NaZn}_2(\text{BH}_4)_5$ was experimentally determined¹⁴ to crystallize in a $P2_1/c$ phase. The lowest-energy structure we discovered by the MHM runs for $\text{NaZn}_2(\text{BH}_4)_5$ belongs to the $I\bar{4}m2$ space group, which is thermodynamically less stable by just 0.2 kJ/mol cation than the $P2_1/c$ phase. The $I\bar{4}m2$ structure for $\text{NaZn}_2(\text{BH}_4)_5$ can also be obtained by relaxing the $I\bar{4}m2$ structure of $\text{LiZn}_2(\text{BH}_4)_5$ after replacing the Li cations by Na cations. Similar to the case of $\text{LiZn}_2(\text{BH}_4)_5$, the $I\bar{4}m2$ consists of one 3D framework while the $P2_1/c$ structure is composed of two inter-penetrated frameworks.¹⁴ The $I\bar{4}m2$ structure is therefore a low-density phase with the density $\rho = 0.54 \text{ g} \times \text{cm}^{-3}$, roughly one half of the density $\rho = 1.15 \text{ g} \times \text{cm}^{-3}$ of the $P2_1/c$ structure. A geometrical illustration for the $P2_1/c$ and $I\bar{4}m2$ phases of $\text{NaZn}_2(\text{BH}_4)_2$ is given in Fig. 6. The density of phonon states of the $I\bar{4}m2$ phase of $\text{NaZn}_2(\text{BH}_4)_5$, as shown in Figure 5(b), indicates that this phase is dynamically stable.

Based on the formation energies, the thermodynamic stability of the structures reported for both $\text{NaZn}(\text{BH}_4)_3$

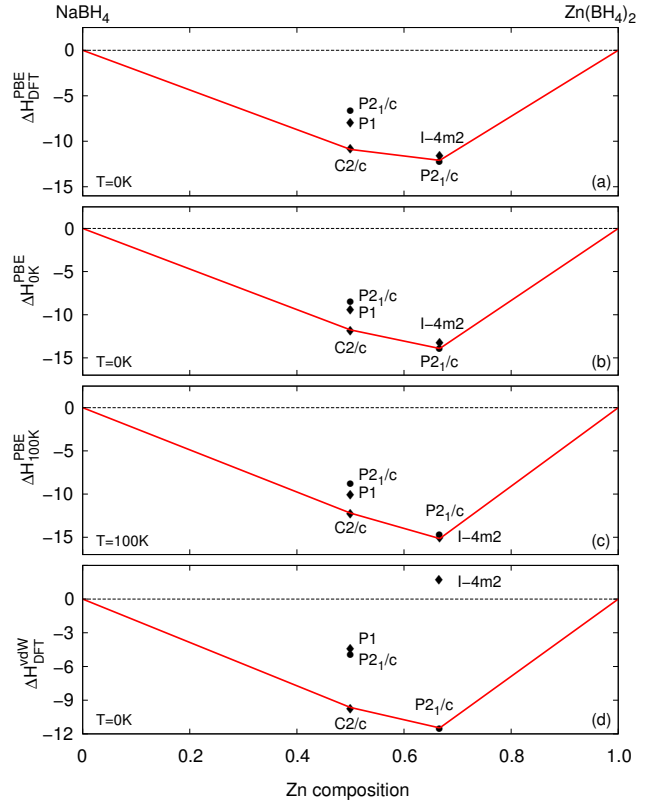


FIG. 7: (Color online) Formation energies $\Delta F_{\text{DFT}}^{\text{PBE}}$, $\Delta F_{0\text{K}}^{\text{PBE}}$, $\Delta F_{100\text{K}}^{\text{PBE}}$, and $\Delta F_{\text{DFT}}^{\text{vdW}}$ (in units of kJ/mol cation) of Na/Zn double-cation borohydrides at 0K and 100K shown vs. Zn composition x . The structures studied are indicated by symbols with the space groups nearby. Diamonds/circles are used for theoretically-predicted/experimentally-reported phases. Constructed from the thermodynamically most stable structures, the red-solid lines form a convex hull, above which all structures are unstable.

and $\text{NaZn}_2(\text{BH}_4)_5$ was examined and presented in Fig. 7. With the PBE functional, the $P2_1/c$ and $I\bar{4}m2$ phases of $\text{NaZn}_2(\text{BH}_4)_5$ are almost degenerate, being the two lowest-energy structures of this compound. For $\text{NaZn}(\text{BH}_4)_3$, $C2/c$ is the lowest-energy structure. At variance from Ref. 18, the formation energy of the $P2_1/c$ phase of $\text{NaZn}(\text{BH}_4)_3$ is always negative, indicating that this phase is stable and would not decompose into NaBH_4 and $\text{Zn}(\text{BH}_4)_2$. In addition, both the $P2_1/c$ and $P1$ structures were found to be unstable with respect to the decomposition into NaBH_4 and $\text{NaZn}_2(\text{BH}_4)_5$. The $C2/c$ phase, on the other hand, was found to be stable.

Similar to the case of Li/Zn borohydrides, the vdW interactions captured by vdW-DF2 calculations play an important role as it lifts the “degeneracy” of the $P2_1/c$ and the $I\bar{4}m2$ structures of $\text{NaZn}_2(\text{BH}_4)_5$. In particular, the formation energy of the $I\bar{4}m2$ structure is slightly positive while $P2_1/c$ is the thermodynamically most stable structure with a strongly negative formation energy.

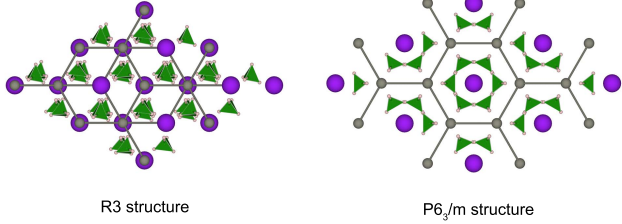


FIG. 8: (Color online) Two low-temperature phases of $\text{KZn}(\text{BH}_4)_3$, the $R3$ phase (left) and $P6_3/m$ phase (right). Potassium and zinc atoms are shown by purple and gray spheres while green tetrahedra represent the $[\text{BH}_4]^-$ anions.

To explain this behavior, we note that the $I\bar{4}m2$ structure consists of one 3D framework while the $P2_1/c$ structure is composed by two inter-penetrated frameworks that are not linked by bonds. The vdW interaction also reverts the energetic ordering of the $P2_1/c$ and the $P1$ structures of $\text{NaZn}(\text{BH}_4)_3$. Moreover, the $C2/c$ phase is again the lowest-energy structure of $\text{NaZn}(\text{BH}_4)_3$ and is stable with respect to the decomposition into NaBH_4 and $\text{NaZn}_2(\text{BH}_4)_5$. This result shows that from the theoretical point of view, the existence of the $C2/c$ phase of $\text{NaZn}(\text{BH}_4)_3$ is possible.

C. Potassium/zinc borohydrides

At 100 K, the experimentally synthesized crystalline $\text{KZn}(\text{BH}_4)_3$ sample was determined¹⁷ to be in a rhombohedral $R3$ phase. A related compound, $\text{KZn}_5(\text{BH}_4)_5$, on the other hand, has not been experimentally identified. Therefore, it would be interesting to explore, in a similar manner to the analysis performed for $\text{LiZn}(\text{BH}_4)_3$, if this hypothetical compound is stable or not. Our MHM runs for $\text{KZn}(\text{BH}_4)_3$ predicted a hexagonal $P6_3/m$ structure (no. 176) to be lowest in the DFT energy with the PBE functional $E_{\text{DFT}}^{\text{PBE}}$. Compared to the $R3$ structure, the $P6_3/m$ structure is thermodynamically more stable by

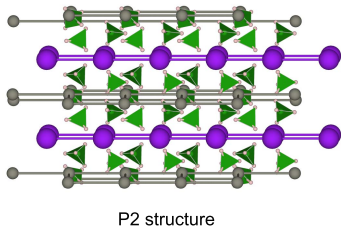


FIG. 9: (Color online) The predicted $P2$ structure of $\text{KZn}_2(\text{BH}_4)_5$. Potassium and zinc atoms are shown by purple and gray spheres while green tetrahedra represent the $[\text{BH}_4]^-$ anions.

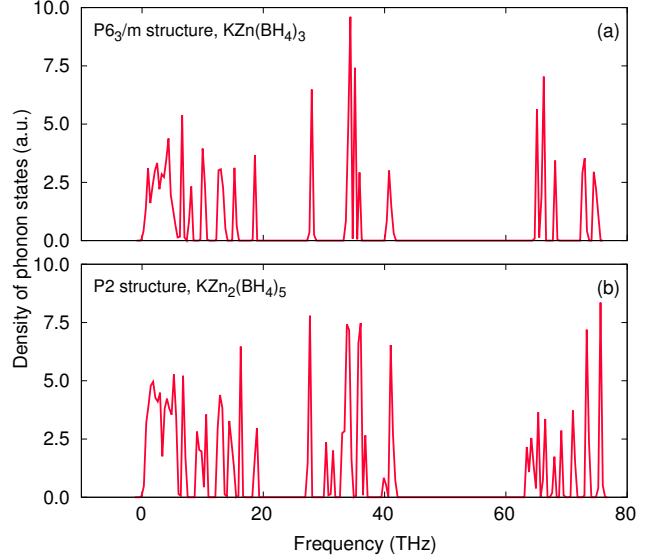


FIG. 10: (Color online) Density of phonon states of (a) the $P6_3/m$ structure of $\text{KZn}(\text{BH}_4)_3$ and (b) the $P2$ structure of $\text{KZn}_2(\text{BH}_4)_5$.

$\simeq 3.5$ kJ/mol cation. The density of the $P6_3/m$ structure is $\rho = 1.05 \text{ g} \times \text{cm}^{-3}$, slightly smaller than that of the $R3$ structure with $\rho = 1.15 \text{ g} \times \text{cm}^{-3}$. For $\text{KZn}_2(\text{BH}_4)_5$, a monoclinic $P2$ structure (no. 3) with $\rho = 1.09 \text{ g} \times \text{cm}^{-3}$ was predicted to be quite low in the DFT energy $E_{\text{DFT}}^{\text{PBE}}$ (see Table II). The geometries of the $P6_3/m$ and $R3$ structures for $\text{KZn}(\text{BH}_4)_3$ are shown in Fig. 8 while the geometry of the $P2$ structure of $\text{KZn}_2(\text{BH}_4)_5$ is shown in Fig. 9. Both the $P6_3/m$ phase of $\text{KZn}(\text{BH}_4)_3$ and the $P2$ phase of $\text{KZn}_2(\text{BH}_4)_5$ were predicted to be dynamically stable, as indicated by Figs. 10(a) and 10(b) for their densities of phonon states.

The thermodynamic stability of the $R3$ and $P6_3/m$ structures of $\text{KZn}(\text{BH}_4)_3$ and the $P2$ structure of $\text{KZn}_2(\text{BH}_4)_5$ was examined and the results are shown in Fig. 11. With the PBE functional, the energies of formation of these structures were determined to be all negative at 0K and 100K, implying that they are stable and would not decompose into KBH_4 and $\text{Zn}(\text{BH}_4)_2$ [see Figs. 11(a)-(c)]. Both the $R3$ and the $P6_3/m$ structures of $\text{KZn}(\text{BH}_4)_3$ are located below the line connecting KBH_4 and the $P2$ phase of $\text{KZn}_2(\text{BH}_4)_5$, thus they are also stable with respect to the decomposition into KBH_4 and $\text{KZn}_2(\text{BH}_4)_5$. Similarly, the $P2$ phase of $\text{KZn}_2(\text{BH}_4)_5$ is stable and would not decompose into $\text{KZn}(\text{BH}_4)_3$ and $\text{Zn}(\text{BH}_4)_2$. Fig. 11(d) indicates that the inclusion of the vdW interactions reverts again the energetic ordering of the $R3$ and the $P6_3/m$ structures of $\text{KZn}(\text{BH}_4)_3$. Consequently, the experimentally reported $R3$ structure is found to be the thermodynamically most stable phase of $\text{KZn}(\text{BH}_4)_3$. For $\text{KZn}_2(\text{BH}_4)_5$, the formation energy of the $P2$ structure remains strongly negative, indicating that this phase is thermodynamically stable. The

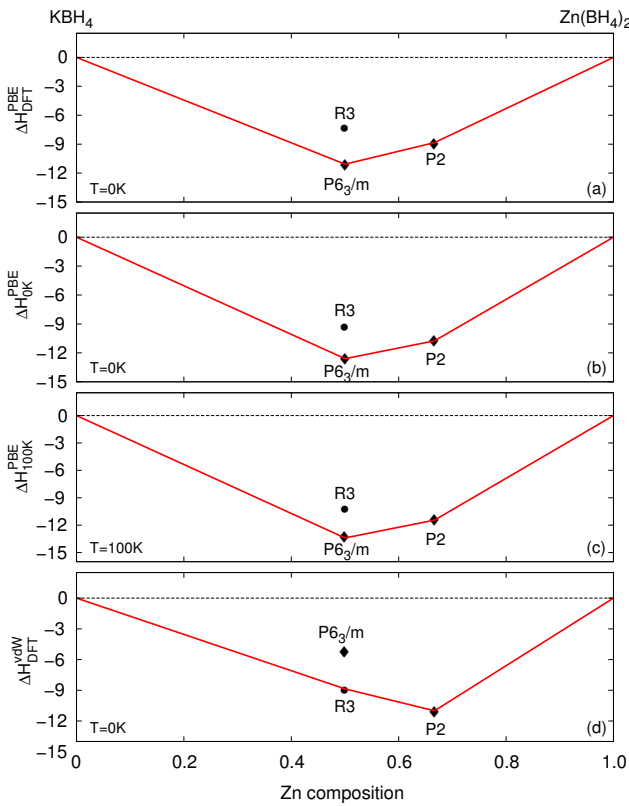


FIG. 11: (Color online) Formation energies $\Delta F_{\text{DFT}}^{\text{PBE}}$, $\Delta F_{0\text{K}}^{\text{PBE}}$, $\Delta F_{100\text{K}}^{\text{PBE}}$, and $\Delta F_{\text{DFT}}^{\text{vdW}}$ (in units of kJ/mol cation) of K/Zn double-cation borohydrides at 0K and 100K shown vs. Zn composition x . The structures studied are indicated by symbols with the space groups nearby. Diamonds/circles are used for theoretically-predicted/experimentally-reported phases. Constructed from the thermodynamically most stable structures, the red-solid lines form a convex hull, above which all structures are unstable.

existence of this hypothetical compound $\text{KZn}_2(\text{BH}_4)_5$ is therefore theoretically possible.

IV. CONCLUSIONS

We performed a systematic study on the thermodynamic stability of a series of Li/Zn, Na/Zn, and K/Zn double-cation borohydrides at low temperatures. Some of them were recently synthesized, others are hypothetical. Using the minima-hopping method, we discovered

two new lowest-energy structures for $\text{NaZn}(\text{BH}_4)_3$, which was experimentally synthesized and $\text{KZn}_2(\text{BH}_4)_5$, a hypothetical compound. The lowest-energy of these compounds, which belong to the $C2/c$ and $P2$ space groups, respectively, are stable with respect to the decomposition into the related compounds, and therefore their existence is predicted. For the hypothetical $\text{LiZn}(\text{BH}_4)_3$ compound, we reach the same conclusion of a previous study¹⁸ that the theoretically proposed $P1$ structure is lowest in energy. We also found that this structure is unstable and would decompose into LiBH_4 and $\text{LiZn}_2(\text{BH}_4)_5$. Therefore, this instability may be the reason why attempts to experimentally identify $\text{LiZn}(\text{BH}_4)_3$ have failed. On the other hand, the experimentally-reported structures of $\text{LiZn}_2(\text{BH}_4)_5$, $\text{NaZn}_2(\text{BH}_4)_5$, and $\text{KZn}(\text{BH}_4)_3$ are also predicted to be the thermodynamically most stable structures.

While lattice vibrations were found to play a minor role in the energetic ordering of the structures studied, van der Waals interactions, on the other hand, seem to be critically important. We found that the PBE functional is not sufficient to capture the non-bonding interactions between the constituent 3D frameworks of the complex structures of $\text{LiZn}_2(\text{BH}_4)_5$ and $\text{NaZn}_2(\text{BH}_4)_5$. Consequently, the energetic ordering of the examined low-energy structures determined at the PBE level is changed. To overcome this problem, we suggest that vdW-DF2, a recently developed non-local density functional, is suitable to access the stability of the low-energy structures of these double-cation borohydrides.

Acknowledgments

The authors thank Radovan Černý for valuable expert discussions. Useful suggestions from Dipulneet Aidhy, Nguyen-Manh Duc, Atsushi Togo, and Aleksey Kolmogorov are appreciated. T. D. H, M. A., and S. G. gratefully acknowledge the financial support from the Swiss National Science Foundation. Work by VNT is supported by the Vietnamese NAFOSTED program No. 103.02-2011.20. L. M. W. gratefully acknowledges financial support from the Department of Energy under Contract No. DE-FG02-06ER46297. The computational work was performed at the Swiss National Supercomputing Center, Hanoi University of Science and Technology, the Research Computing at the University of South Florida, and École Polytechnique Fédérale de Lausanne.

* Electronic address: stefan.goedecker@unibas.ch

¹ A. Züttel and L. Schlapbach, *Nature (London)* **414**, 353 (2001).

² T. K. Mandal and D. H. Gregory, *Annu. Rep. Prog. Chem., Sect. A* **105**, 21 (2009).

³ B. Sakintuna, F. Lamari-Darkrim, and M. Hirscher, *Int. J. Hydrogen Energy* **32**, 1121 (2007).

⁴ I. Jain, P. Jain, and A. Jain, *J. Alloys Compd.* **503**, 303 (2010).

⁵ L. H. Rude, T. K. Nielsen, D. B. Ravnsbæk, U. Bösenberg,

M. B. Ley, B. Richter, L. M. Arnbjerg, M. Dornheim, Y. Filinchuk, F. Besenbacher, and T. R. Jensen, *Phys. Status Solidi A* **208**, 1754 (2011).

⁶ E. A. Nickels, M. O. Jones, W. I. F. David, S. R. Johnson, R. L. Lowton, M. Sommariva, and P. P. Edwards, *Angew. Chem. Int. Ed.* **47**, 2817 (2008).

⁷ Z.-Z. Fang, X.-D. Kang, J.-H. Luo, P. Wang, H.-W. Li, and S.-i. Orimo, *J. Phys. Chem. C* **114**, 22736 (2010).

⁸ H. Hagemann, M. Longhini, J. W. Kaminski, T. A. Wesolowski, R. Černý, N. Penin, M. H. Sørby, B. C. Hauback, G. Severa, and C. M. Jensen, *J. Phys. Chem. A* **112**, 7551 (2008).

⁹ R. Černý, G. Severa, D. B. Ravnsbæk, Y. Filinchuk, V. D'Anna, H. Hagemann, D. Haase, C. M. Jensen, and T. R. Jensen, *J. of Phys. Chem. C* **114**, 1357 (2010).

¹⁰ R. Černý, D. B. Ravnsbæk, G. Severa, Y. Filinchuk, V. D' Anna, H. Hagemann, D. Haase, J. Skibsted, C. M. Jensen, and T. R. Jensen, *J. Phys. Chem. C* **114**, 19540 (2010).

¹¹ I. Lindemann, R. D. Ferrer, L. Dunsch, R. Černý, H. Hagemann, V. D'Anna, Y. Filinchuk, L. Schultz, and O. Gutfleisch, *Faraday Discuss.* **151**, 231 (2011).

¹² P. Schouwink, V. D'Anna, M. B. Ley, L. M. Lawson Daku, B. Richter, T. R. Jensen, H. Hagemann, and R. Černý, *J. Phys. Chem. C* **116**, 10829 (2012).

¹³ T. Jarón and W. Grochala, *Dalton Trans.* **40**, 12808 (2011).

¹⁴ D. Ravnsbæk, Y. Filinchuk, Y. Cerenius, H. J. Jakobsen, F. Besenbacher, J. Skibsted, and T. R. Jensen, *Angew. Chem. Int. Ed.* **48**, 6659 (2009).

¹⁵ R. Černý, K. Chul Kim, N. Penin, V. D'Anna, H. Hagemann, and D. S. Sholl, *J. Phys. Chem. C* **114**, 19127 (2010).

¹⁶ D. B. Ravnsbæk, C. Frommen, D. Reed, Y. Filinchuk, M. Sørby, B. C. Hauback, H. Jakobsen, D. Book, F. Besenbacher, J. Skibsted, and T. Jensen, *J. Alloys Compd.* **509**, S698 (2011).

¹⁷ R. Černý, D. B. Ravnsbæk, P. Schouwink, Y. Filinchuk, N. Penin, J. Teyssier, L. Smrčok, and T. R. Jensen, *J. Phys. Chem. C* **116**, 1563 (2012).

¹⁸ D. S. Aidhy and C. Wolverton, *Phys. Rev. B* **83**, 144111 (2011).

¹⁹ X.-B. Xiao, W.-Y. Yu, and B.-Y. Tang, *J. Phys.: Condens. Matter* **20**, 445210 (2008).

²⁰ L. W. Huang, O. Elkedi, and X. Li, *J. Alloys Compd.* **536**, (2011).

²¹ K. C. Kim, *Int. J. Quantum Chem.* **113**, 119 (2013).

²² K. C. Kim, *J. Chem. Phys.* **137**, 084111 (2012).

²³ S. Goedecker, *J. Chem. Phys.* **120**, 9911 (2004).

²⁴ M. Amsler and S. Goedecker, *J. Chem. Phys.* **133**, 224104 (2010).

²⁵ A. Bil, B. Kolb, R. Atkinson, D. G. Pettifor, T. Thonhauser, and A. N. Kolmogorov, *Phys. Rev. B* **83**, 224103 (2011).

²⁶ M. Dion, H. Rydberg, E. Schroder, D. C. Langreth, and B. I. Lundqvist, *Phys. Rev. Lett.* **92**, 246401 (2004).

²⁷ T. Thonhauser, V. R. Cooper, S. Li, A. Puzder, P. Hyldgaard, and D. C. Langreth, *Phys. Rev. B* **76**, 125112 (2007).

²⁸ G. Roman-Perez and J. M. Soler, *Phys. Rev. Lett.* **103**, 096102 (2009).

²⁹ K. Lee, É. D. Murray, L. Kong, B. I. Lundqvist, and D. C. Langreth, *Phys. Rev. B* **82**, 081101(R) (2010).

³⁰ P. Hohenberg and W. Kohn, *Phys. Rev.* **136**, (1964).

³¹ W. Kohn and L. Sham, *Phys. Rev.* **140**, (1965).

³² J. P. Perdew, K. Burke, and M. Ernzerhof, *Phys. Rev. Lett.* **77**, 3865 (1996).

³³ P. E. Blöchl, *Phys. Rev. B* **50**, 17953 (1994).

³⁴ G. Kresse and J. Furthmüller, *Phys. Rev. B* **54**, 11169 (1996).

³⁵ G. Kresse and Furthmüller, *J. Comput. Mater. Sci.* **6**, 15 (1996).

³⁶ G. Kresse and J. Hafner, *Phys. Rev. B* **47**, 558 (1993).

³⁷ H. J. Monkhorst and J. D. Pack, *Phys. Rev. B* **13**, 5188 (1976).

³⁸ P. Giannozzi, S. Baroni, N. Bonini, M. Calandra, R. Car, C. Cavazzoni, D. Ceresoli, G. L. Chiarotti, M. Cococcioni, I. Dabo, A. D. Corso, S. d. Gironcoli, S. Fabris, G. Fratesi, R. Gebauer, U. Gerstmann, C. Gougonnissis, A. Kokalj, M. Lazzeri, L. Martin-Samos, N. Marzari, F. Mauri, R. Mazzarello, S. Paolini, A. Pasquarello, L. Paulatto, C. Sbraccia, S. Scandolo, G. Sclauzero, A. P. Seitsonen, A. Smogunov, P. Umari, and R. M. Wentzcovitch, *J. Phys.: Condens. Matter* **21**, 395502 (2009).

³⁹ J. P. Perdew and Y. Wang, *Phys. Rev. B* **33**, 8800 (1986).

⁴⁰ E. D. Murray, K. Lee, and D. C. Langreth, *Journal of Chemical Theory and Computation* **5**, 2754 (2009).

⁴¹ FINDSYM, <http://stokes.byu.edu/findsym.html>.

⁴² K. Momma and F. Izumi, *J. Appl. Crystallogr.* **41**, 653 (2008).

⁴³ J.-P. Soulié, G. Renaudin, R. Černý, and K. Yvon, *J. Alloys Compd.* **346**, 200 (2002).

⁴⁴ P. Fischer and A. Zuettel, *Mater. Sci. Forum.* **443-444**, 287 (2004).

⁴⁵ P. T. Ford and H. M. Powell, *Acta Cryst.* **7**, 604 (1954).

⁴⁶ P. Vajeeston, P. Ravindran, A. Kjekshus, and H. Fjellvåg, *J. Alloys Compd.* **387**, 97 (2005).

⁴⁷ D. S. Aidhy, 2012, private communication.

⁴⁸ R. Černý, 2013, private communication.

⁴⁹ W. Hellmann, R. G. Hennig, S. Goedecker, C. J. Umrigar, B. Delley, and T. Lenosky, *Phys. Rev. B* **75**, 085411 (2007).

⁵⁰ S. Roy, S. Goedecker, M. J. Field, and E. Penev, *J. Phys. Chem. B* **113**, 7315 (2009).

⁵¹ K. Bao, S. Goedecker, K. Koga, F. Lançon, and A. Neelov, *Phys. Rev. B* **79**, 041405 (2009).

⁵² A. Willand, M. Gramzow, S. AlirezaGhasemi, L. Genovese, T. Deutsch, K. Reuter, and S. Goedecker, *Phys. Rev. B* **81**, 201405 (2010).

⁵³ S. De, A. Willand, M. Amsler, P. Pochet, L. Genovese, and S. Goedecker, *Phys. Rev. Lett.* **106**, 225502 (2011).

⁵⁴ M. Amsler, J. A. Flores-Livas, L. Lehtovaara, F. Balima, S. A. Ghasemi, D. Machon, S. Pailhès, A. Willand, D. Caliste, S. Botti, A. SanMiguel, S. Goedecker, and M. A. L. Marques, *Phys. Rev. Lett.* **108**, 065501 (2012).

⁵⁵ J. A. Flores-Livas, M. Amsler, T. J. Lenosky, L. Lehtovaara, S. Botti, M. A. L. Marques, and S. Goedecker, *Phys. Rev. Lett.* **108**, 117004 (2012).

⁵⁶ M. Amsler, J. A. Flores-Livas, T. D. Huan, S. Botti, M. A. L. Marques, and S. Goedecker, *Phys. Rev. Lett.* **108**, 205505 (2012).

⁵⁷ T. D. Huan, M. Amsler, V. N. Tuoc, A. Willand, and S. Goedecker, *Phys. Rev. B* **86**, 224110 (2012).

⁵⁸ T. D. Huan, M. Amsler, M. A. L. Marques, S. Botti, A. Willand, and S. Goedecker, *Phys. Rev. Lett.* **110**, 135502 (2013).

⁵⁹ M. Haertelt, J. T. Lyon, P. Vlaes, J. de Haeck, P. Lievens, and A. Fielicke, *J. Chem. Phys.* **136**, 064301 (2012).

⁶⁰ V. P. Markevich, A. R. Peaker, S. B. Lastovskii, L. I. Murin, J. Coutinho, V. J. B. Torres, P. R. Briddon, L. Dobaczewski, E. V. Monakhov, and B. G. Svensson, Phys. Rev. B **80**, 235207 (2009).

⁶¹ A. Togo, F. Oba, and I. Tanaka, Phys. Rev. B **78**, 134106 (2008).

⁶² K. Parlinski, Z.-Q. Li, and Y. Kawazoe, Phys. Rev. Lett. **78**, 4063 (1997).

⁶³ L. G. Hector, Jr., J. F. Herbst, W. Wolf, P. Saxe, and G. Kresse, Phys. Rev. B **76**, 014121 (2007).

⁶⁴ J. F. Herbst, L. G. Hector, Jr., and W. Wolf, Phys. Rev. B **82**, 024110 (2010).

⁶⁵ E. Jeon and Y. Cho, J. Alloys Compd. **422**, 273 (2006).

⁶⁶ S. Srinivasan, D. Escobar, M. Jurczyk, Y. Goswami, and E. Stefanakos, J. Alloys Compd. **462**, 294 (2008).

⁶⁷ A. Züttel, A. Borgschultea, and S.-I. Orimo, Scripta Materialia **56**, 823 (2007).

⁶⁸ See supplemental material for additional information reported in this work.

⁶⁹ J. Rodríguez-Carvajal, Physica B **192**, 55 (1993).

Supplemental Material: Thermodynamic stability of alkali metal/zinc double-cation borohydrides at low temperatures

Tran Doan Huan,¹ Maximilian Amsler,¹ Riccardo Sabatini,² Vu Ngoc Tuoc,³ Nam Ba Le,⁴ Lilia M. Woods,⁴ Nicola Marzari,² and Stefan Goedecker^{1,*}

¹*Department of Physics, Universität Basel, Klingelbergstrasse 82, 4056 Basel, Switzerland*

²*Theory and Simulation of Materials, École Polytechnique Fédérale de Lausanne, Station 12, 1015 Lausanne, Switzerland*

³*Institute of Engineering Physics, Hanoi University of Science and Technology, 1 Dai Co Viet Road, Hanoi, Vietnam*

⁴*Department of Physics, University of South Florida, 4202 E. Fowler Ave., Tampa, FL 33620, USA*

(Dated: April 16, 2013)

TABLE I – continued from previous page

K	2b	0.00000	0.00000	0.00000
Zn	2c	0.33333	0.66667	0.25000
B	6h	0.18024	0.36048	0.25000
H	12i	-0.22693	-0.45387	-0.11496
H	6h	-0.27308	-0.01277	0.25000
H	6h	-0.27307	-0.26031	0.25000

P2 phase, KZn₂(BH₄)₅

a = 7.146 Å, b = 5.130 Å, c = 10.151 Å

α = γ = 90°, β = 88.741°

Atom	WP	x	y	z
K	1c	0.50000	-0.28780	0.00000
Zn	2e	-0.04620	0.09929	-0.28148
B	2e	0.29681	0.25477	0.17862
B	1b	0.00000	0.16741	0.50000
B	2e	0.16888	-0.14806	-0.19612
H	2e	0.31447	0.22295	0.06063
H	2e	0.12578	0.02371	0.45644
H	2e	0.14255	-0.21993	-0.08374
H	2e	0.41437	0.38313	0.23277
H	2e	-0.07793	0.31402	0.42239
H	2e	-0.14432	0.37736	-0.19422
H	2e	0.17621	0.09776	-0.19369
H	2e	0.29818	0.03408	0.23206
H	2e	0.30971	-0.21894	-0.25384
H	2e	0.03511	-0.23848	-0.26096

I4m2 phase, LiZn₂(BH₄)₅

a = b = 8.396 Å, c = 16.926 Å

α = β = γ = 90°

Atom	WP	x	y	z
Li	2d	0.00000	0.50000	0.75000
Zn	4e	0.00000	0.00000	0.13400
B	8i	-0.23449	0.00000	0.18952
B	2a	0.00000	0.00000	0.00000
H	16j	0.37333	0.33797	0.32746
H	8i	0.35451	0.00000	0.14971
H	8i	0.12618	0.00000	-0.03731
H	8i	-0.24850	0.00000	0.26071

C2/c phase, NaZn(BH₄)₃

a = 7.793 Å, b = 15.723 Å, c = 7.680 Å

α = γ = 90°, β = 110.418°

Atom	WP	x	y	z
Na	4e	0.00000	-0.05711	0.25000
Zn	4e	0.00000	-0.37109	0.25000
B	8f	-0.24773	0.04904	0.33521
B	4e	0.00000	-0.23185	0.25000
H	8f	0.23169	0.47318	0.30728
H	8f	-0.09158	0.07548	0.40084
H	8f	-0.31184	0.08602	0.18126
H	8f	-0.32512	0.06702	0.44784
H	8f	-0.36324	0.30786	0.26099
H	8f	-0.46155	0.22504	0.39673

I4m2 phase, NaZn₂(BH₄)₅

a = b = 8.863 Å, c = 17.823 Å

α = β = γ = 90°

Atom	WP	x	y	z
Na	2d	0.00000	0.50000	0.75000
Zn	4e	0.00000	0.00000	0.12723
B	8i	-0.22178	0.00000	0.18054
B	2a	0.00000	0.00000	0.00000
H	16j	-0.38010	-0.34645	0.33640
H	8i	0.33654	0.00000	0.14357
H	8i	0.11954	0.00000	-0.03543
H	8i	-0.23158	0.00000	0.24830

P6₃/m phase, KZn(BH₄)₃

a = b = 8.361 Å, c = 7.820 Å

α = β = 90°, γ = 120°

Atom	WP	x	y	z
to be continued ...				

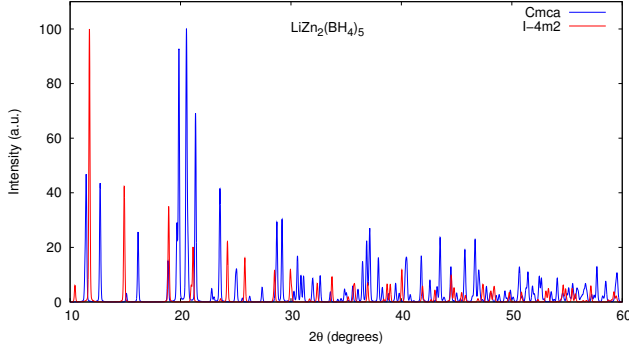


FIG. 1: (Color online) Simulated XRD patterns of the $Cmca$ and $I\bar{4}m2$ phases of $\text{LiZn}_2(\text{BH}_4)_5$.

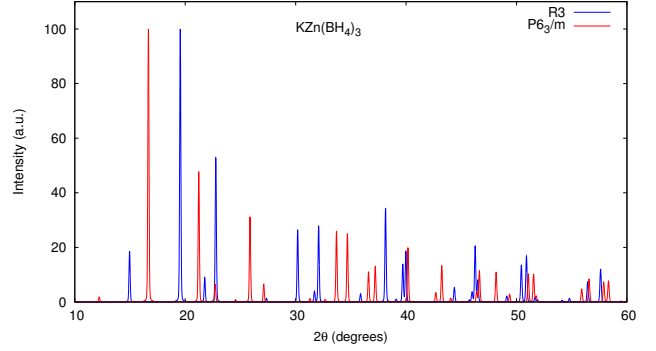


FIG. 4: (Color online) Simulated XRD patterns of the $R3$ and $P6_3/m$ phases of $\text{KZn}(\text{BH}_4)_3$.

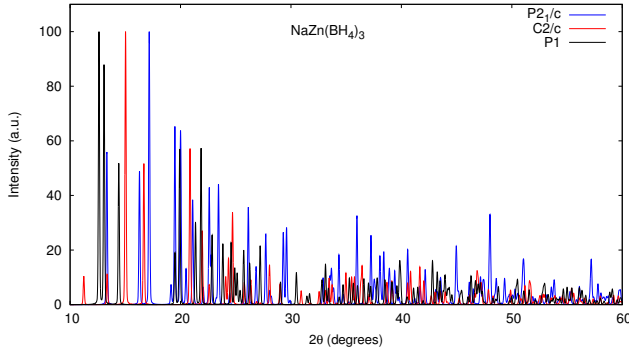


FIG. 2: (Color online) Simulated XRD patterns of the $P2_1/c$, $C2/c$, and $P1$ phases of $\text{NaZn}(\text{BH}_4)_3$.

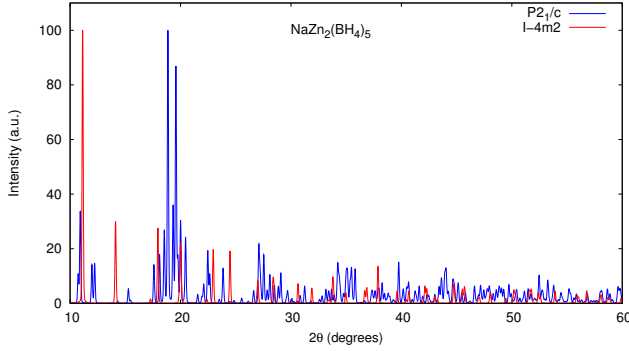


FIG. 3: (Color online) Simulated XRD patterns of the $P2_1/c$ and $I\bar{4}m2$ phases of $\text{NaZn}_2(\text{BH}_4)_5$.

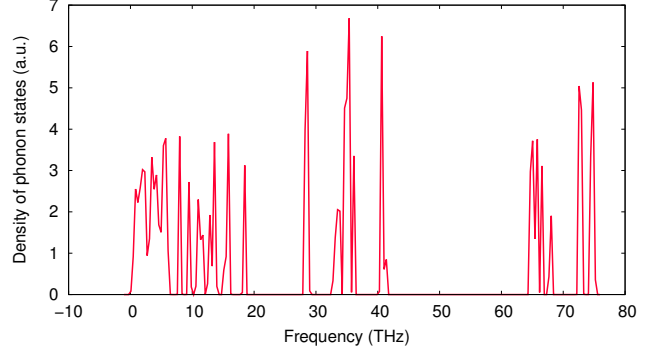


FIG. 5: (Color online) Density of phonon states of the $P1$ phase proposed for $\text{NaZn}(\text{BH}_4)_3$.

* Electronic address: stefan.goedecker@unibas.ch